REPORT 962

THE AERODYNAMIC FORCES ON SLENDER PLANE- AND CRUCIFORM-WING AND BODY COMBINATIONS

By JOHN R. SPREITER

SUMMARY

The load distribution, forces, and moments are calculated theoretically for inclined slender wing-body combinations consisting of a slender body of revolution and either a plane or cruciform arrangement of low-aspect-ratio pointed wings. The results are applicable at subsonic and transonic speeds, and at supersonic speeds, provided the entire wing-body combination lies near the center of the Mach cone.

The analysis of the slender cruciform-wing and body combinations results in the following conclusions: The lift and pitching moment are independent of the angle of yaw, and the side force and yawing moment are independent of the angle of attack. If the vertical and horizontal wings are identical, the rolling moment is zero for all angles of pitch and yaw. By symmetry considerations, these results are shown to be equally applicable for any cruciform-wing and body combination having identical horizontal and vertical wings of arbitrary plan form and aspect ratio.

INTRODUCTION

A great amount of research is being conducted on aircraft configurations that may be described as slender wing-body combinations, that is, a wing-body combination consisting of a slender pointed body and pointed low-aspect-ratio wings. Although the aerodynamic characteristics of the components may be well known, the mutual interference resulting from their combination may be so great that it is desirable to study the aerodynamic properties of the complete configuration. The mutual interference, in an incompressible medium, of a fuselage and a wing of high aspect ratio (to which lifting-line theory is applicable) has been investigated by Lennertz, Wieselsberger, Pepper, and Multhopp in references 1, 2, 3, and 4. Since these results were not applicable to the present problem, a theoretical analysis of the aerodynamic properties of slender wing-body combinations was undertaken. The results of this investigation were first reported in reference 5 and were later extended in reference 6 to include cruciform-wing and body combinations. The present report summarizes and extends the theory and results previously presented in these references.

The aerodynamic properties of slender wing-body combinations may be approximated by the method originally used by Munk in studying the aerodynamics of slender airships (reference 7). R. T. Jones (reference 8) extended this method to the study of low-aspect-ratio pointed wings and Ribner (reference 9) applied it to determine the stability derivatives of low-aspect-ratio triangular wings. The essential point in the study of slender bodies by this method is the fact that the flow in the vicinity of the body is approximately two-dimensional when viewed in planes perpendicular to the direction of motion.

This theory is applied first to plane-wing and body combinations inclined at small angles of attack. For this portion of the analysis the wings must have a pointed leading apex, a swept-back leading edge, and such a plan form that no part of the trailing edge extends forward of the station of maximum span. The theory is next applied to cruciform-wing and body combinations inclined at small angles in yaw and pitch. In addition to the restrictions mentioned previously, it is necessary, for this case, to specify that the trailing edges of the wings are unswept. The results of this analysis are applicable to combinations having very low-aspect-ratio wings at all Mach numbers or to combinations having wings of moderate aspect ratio at Mach numbers near 1. Examples are included to illustrate the calculation of the load distribution, forces, and moments on several elementary wing-body combinations having either plane or cruciform wings.

The analysis of slender cruciform-wing and body combinations resulted in the discovery of certain general characteristics of combinations having identical horizontal and vertical wings complying, of course, with all the requirements of slender wing-body theory. To ascertain whether all these requirements were necessary, an investigation of the forces and moments of cruciform-wing and body combinations having identical wings was made on the basis of symmetry considerations. It was found that, within the limitations of linear theory, these particular conclusions were valid for all cruciform-wing and body combinations regardless of the plan form or aspect ratio of the wing.

SYMBOLS

A	aspect ratio $\left(\frac{\text{maximum span squared}}{\text{area}}\right)$
B	cross-section area of body of revolution (πa^2)
B_b	cross-section area of base of body of revolution
B_m	mean cross-section area of body of revolution $\left(\frac{\text{volume}}{\text{length}}\right)$
C_L	lift coefficient $\left(\frac{L}{qS_H}\right)$
C_l	rolling-moment coefficient $\left(\frac{L'}{2qS_H s_0}\right)$

C_m pitching-moment coefficient $\left(\frac{M}{qS_Hc_H}\right)$

C_n yawing-moment coefficient $\left(\frac{N}{qS_Vc_V}\right)$

C_Y side-force coefficient $\left(\frac{Y}{qS_V}\right)$

L lift

L' rolling moment

L'_L rolling moment due to lifting forces

L'_Y rolling moment due to side forces

M pitching moment about leading edge of root chord of horizontal wing

M_0 free-stream Mach number

N yawing moment about leading edge of root chord of vertical wing

S wing area

V_0 free-stream velocity

W complex potential function $(\phi+i\psi)$

X complex variable $(y+iz)$

Y side force

a radius of body

a_0 maximum radius of body

c root chord of wing

c' effective wing chord

d semispan of flat plate

i imaginary unit $(\sqrt{-1})$

l length of the portion of the body forward of the wing

p static pressure

Δp_L local pressure difference between lower and upper surfaces

Δp_Y local pressure difference between port and starboard surfaces

q free-stream dynamic pressure

r, θ polar coordinates

s local semispan of horizontal wing

s_0 maximum semispan of horizontal wing

t local semispan of vertical wing

t_0 maximum semispan of vertical wing

u perturbation velocity component in the free-stream direction

$x, y, z,$ Cartesian coordinates

$(x_{c.p.})_L$ distance from leading edge of root chord of horizontal wing to center of pressure of lifting forces

$(x_{c.p.})_Y$ distance from leading edge of root chord of vertical wing to center of pressure of side forces

Φ angle of bank

ψ stream function

α angle of attack

β angle of sideslip

η, ζ transformed rectangular coordinates

ξ complex variable $(\eta+i\zeta)$

ρ density of air

ϕ perturbation velocity potential

ϕ' perturbation velocity potential corresponding to unit angles of pitch or yaw

SUBSCRIPTS

B body

H horizontal wing

V vertical wing

W basic wing without body

a pertains to angle-of-attack case having zero yaw

b pertains to sideslip case having zero angle of attack

l lower side

p port side

s starboard side

u upper side

ANALYSIS

The prime problem to be treated in this report is the prediction of the load distribution, forces, and moments on inclined slender wing-body combinations traveling at subsonic, sonic, or supersonic speeds. In the major portion of the analysis, it is assumed that the bodies are slender bodies of revolution and that the wings have pointed leading apexes, highly swept-back leading edges, and plan forms such that no part of the trailing edge lies forward of the station of maximum span. The wing plan forms are otherwise arbitrary. In certain special cases, however, these requirements will be relaxed so as to include wings of arbitrary aspect ratio and sweep. The study will consist essentially of two parts: The first will be devoted to plane-wing and body combinations each consisting of a body of revolution and a horizontal wing; the second, to cruciform-wing and body combinations each consisting of a body of revolution and a cruciform arrangement of horizontal and vertical wings. In the latter section, the horizontal and vertical wings may be of different plan form and size.

The principal approach to the problem will be based on the general arguments advanced in references 7, 8, and 5 for slender bodies, wings, and wing-body combinations. The assumptions involved in the study of these configurations permit the Prandtl linearized differential equation for the pertubation velocity potential of a compressible flow in three dimensions

$$(1-M_0^2)\phi_{xx}+\phi_{yy}+\phi_{zz}=0 \tag{1}$$

to be reduced to a particularly simple parabolic differential equation in three dimensions

$$\phi_{yy}+\phi_{zz}=0 \tag{2}$$

The slender-body and low-aspect-ratio wing theories (references 7 and 8) neglect the term $(1-M_0^2)\phi_{xx}$ in comparison with ϕ_{yy} and ϕ_{zz} because ϕ_{xx} is very small for slender wings and bodies. Therefore, the loading and aerodynamic properties of plan forms having very low aspect ratios are independent of Mach number. As pointed out in reference 5 and discussed in greater detail in reference 10, the theory is also valid for swept-back plan forms of moderate aspect ratio at sonic velocity, since the term $(1-M_0^2)\phi_{xx}$ can be neglected because $1-M_0^2$ is zero, provided that ϕ_{xx} does not become very large in comparison with the other velocity gradients ϕ_{yy} and ϕ_{zz}. In both the low-aspect-ratio and sonic applications, it should be noted that, with the exception of the infinitely long swept wing, it is possible to solve only problems involving the differential pressure arising from an asymmetry of the flow field. Thus, lifting problems may be treated satisfactorily; whereas, in general, thickness problems cannot. If a thickness problem is attempted by

this method, however, it will be found that the theory predicts infinite longitudinal perturbation velocities and hence infinite pressures at all points on the surfaces of wings and bodies other than the infinitely long swept wing.

The form of equation (2) permits the analysis to be undertaken as a two-dimensional potential-flow problem at this point; each vertical plane, therefore, may be treated independently of the adjacent planes in the determination of the velocity potential. Thus, the potential is determined for an arbitrary $x=x_0$ plane; then, since the x_0 plane may represent any plane normal to the fuselage center line, the potential distribution is known for the entire wing-body combination.

SLENDER PLANE-WING AND BODY COMBINATIONS

THEORY

The first problems to be considered in this report are those related to slender plane-wing and body combinations inclined at small angles of attack. Such a wing-body combination is considered to consist of a slender body of revolution and a flat highly swept-back low-aspect-ratio wing extending along the continuation of the horizontal meridian plane of the body. (See fig. 1.) These problems may be

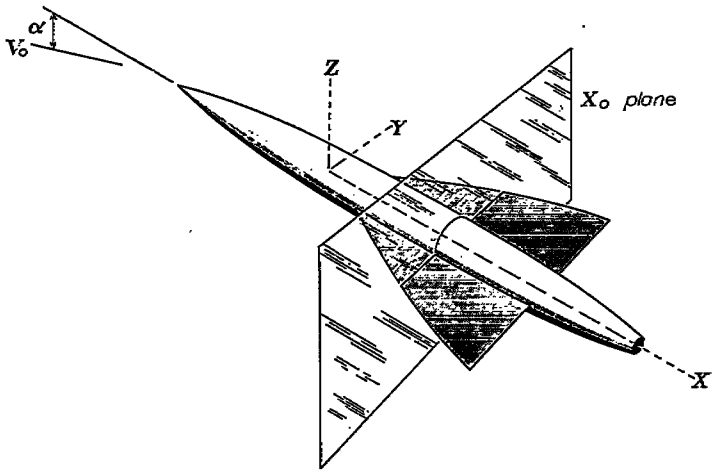

FIGURE 1.—View of plane-wing and body combination showing coordinate axes.

treated by determining the perturbation velocity potential ϕ by means of equation (2) together with the following boundary conditions:
at the surface of the wing

$$\frac{\partial\phi}{\partial z}=0 \tag{3}$$

at the surface of the body

$$\frac{\partial\phi}{\partial r}=0 \tag{4}$$

infinitely far ahead or to the side of the wing-body combination

$$\text{grad } \phi=\bar{k}V_0\alpha$$

where $\bar{k}$ is the unit vector in the z direction and finally ϕ is continuous everywhere except across the surface of the wing-body combination or its wake.

Velocity potential.—As a consequence of the differential equation and the boundary conditions, the perturbation velocity field in the x_0 plane at any station forward of the station of maximum span is similar to the velocity field around an infinitely long cylinder, the cross section of which corresponds to the trace of the wing-body combination in the x_0 plane. For a slender plane-wing and body combination inclined an angle α in pitch, the flow in the x_0 plane is as shown in figure 2 (a) where the flow velocity at infinity is

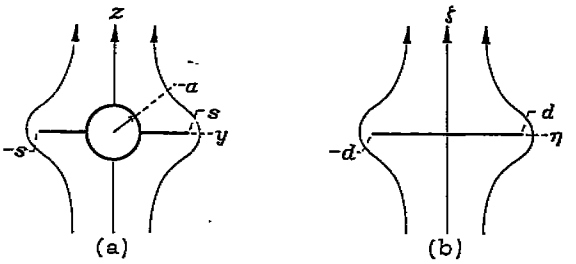

FIGURE 2.—Two-dimensional flow fields corresponding to plane-wing and body combination.

in the direction of the positive z axis and has a velocity of $V_0\alpha$. The flow around a section such as shown in figure 2(a) may be derived from the transverse flow around an infinitely long flat plate (fig. 2(b)) by application of the principles of conformal mapping using the Joukowski transformation. Thus, we consider the mapping of the $\eta\zeta$ plane of figure 2(b) onto the yz plane of figure 2(a) by the relation

$$\xi=X+\frac{a^2}{X} \tag{6}$$

where

$$\xi=\eta+i\zeta$$

and

$$X=y+iz$$

The complex potential function for the flow in the $\eta\zeta$ plane is (see, for instance, reference 11, p. 66)

$$W_a=\phi_a+i\psi_a=-iV_0\alpha\sqrt{\xi^2-d^2} \tag{7}$$

If $d=2a$, the flow around a flat plate expressed by equation (7) transforms by equation (6) into the vertical flow around a circle of radius a having its center at the origin. If d is taken larger than $2a$, the flat-plate flow transforms into the desired vertical flow around a cylinder consisting of a circular cylinder of radius a with thin flat plates extending outward along the extension of the horizontal diameter to a distance s from the origin. When the $\eta\zeta$ plane is transformed into the yz plane in this manner, the complex potential for the flow in the yz plane is found to be

$$W_a=\phi_a+i\psi_a=-iV_0\alpha\sqrt{\left(X+\frac{a^2}{X}\right)^2-d^2}$$

$$=-iV_0\alpha\sqrt{\left(X+\frac{a^2}{X}\right)^2-\left(s+\frac{a^2}{s}\right)^2} \tag{8}$$

since the point d in the $\eta\zeta$ plane corresponds to the point s in the yz plane. The velocity potential ϕ_a for the flow in the yz plane may then be found by squaring equation (8),

substituting $X=r(\cos\theta+i\sin\theta)$, and solving. Thus is obtained

$$\phi_a=\pm\frac{V_0\alpha}{\sqrt{2}}\left\{\left[-\left(1+\frac{a^4}{r^4}\right)r^2\cos 2\theta+s^2\left(1+\frac{a^4}{s^4}\right)\right]+\left[r^4\left(1-\frac{a^4}{r^4}\right)^2+4a^4\cos^2 2\theta+s^4\left(1+\frac{a^4}{s^4}\right)^2-2s^2\left(1+\frac{a^4}{s^4}\right)\left(1+\frac{a^4}{r^4}\right)r^2\cos 2\theta\right]^{\frac{1}{2}}\right\}^{\frac{1}{2}} \quad (9)$$

where the sign is positive in the upper half plane $0<\theta<\pi$ and negative in the lower half plane $\pi<\theta<2\pi$.

Load distribution.—The lifting differential pressure coefficient in linearized potential flow is given by

$$\frac{\Delta p_L}{q}=\frac{2\Delta u_L}{V_0}=\frac{2(u_u-u_l)}{V_0}=\frac{2}{V_0}\Delta\frac{\partial\phi_L}{\partial x}=\frac{2}{V_0}\left(\Delta\frac{\partial\phi_L}{\partial s}\frac{ds}{dx}+\Delta\frac{\partial\phi_L}{\partial a}\frac{da}{dx}\right) \quad (10)$$

where Δ represents the difference in values between corresponding points on the upper and lower surfaces of the wing-body combination. The load distribution may now be determined by substituting the expression for the velocity potential given in equation (9) into equation (10) and letting ϕ equal 0 or ϕ equal π for the wing loading and r equal a for the body loading. The loading over the wing is then found to be given by

$$\left(\frac{\Delta p_L}{q}\right)_H=4\alpha\left\{\frac{\frac{ds}{dx}\left(1-\frac{a^4}{s^4}\right)+\frac{da}{dx}\left[2\frac{a}{s}\left(\frac{a^2}{s^2}-\frac{a^2}{r^2}\right)\right]}{\sqrt{\left(1+\frac{a^4}{s^4}\right)-\frac{r^2}{s^2}\left(1+\frac{a^4}{r^4}\right)}}\right\} \quad (11)$$

and that over the body is given by

$$\left(\frac{\Delta p_L}{q}\right)_B=4\alpha\left[\frac{\frac{ds}{dx}\left(1-\frac{a^4}{s^4}\right)+2\frac{a}{s}\frac{da}{dx}\left(1+\frac{a^2}{s^2}-2\frac{y^2}{a^2}\right)}{\sqrt{\left(1+\frac{a^2}{s^2}\right)^2-4\frac{y^2}{s^2}}}\right] \quad (12)$$

It should be remembered that equations (11) and (12) are valid only at stations forward of the station of maximum wing span. To extend the solutions to stations farther aft, consideration must be given to the influence of the vortex wake trailing from all portions of the trailing edge of the wing that lie aft of the station of maximum span. This point will be discussed at greater length in the application of the theory to specific configurations.

Total forces and moments.—The total lift and pitching moment of a complete wing-body combination may be determined by integrating the loading over the entire planform area. Expressed in nondimensional form, these characteristics are given by

$$C_L=\frac{1}{S_H}\int\int\left(\frac{\Delta p_L}{q}\right)dx\,dy \quad (13)$$

$$C_m=-\frac{1}{S_Hc_H}\int\int\left(\frac{\Delta p_L}{q}\right)x\,dx\,dy \quad (14)$$

$$\frac{x_{c.p.}}{c_H}=-\frac{C_m}{C_L} \quad (15)$$

where S_H is the reference area, c_H is the reference chord or length, and the integration is carried over the complete plan form. It is often convenient to carry out the integration by first evaluating the lift on one spanwise strip and then integrating these elemental lift forces over the length of the wing-body combination, thus

$$\frac{d}{dx}\left(\frac{L}{q}\right)=\int_{-s}^{+s}\left(\frac{\Delta p_L}{q}\right)dy=4\pi\alpha s\left[\frac{ds}{dx}\left(1-\frac{a^4}{s^4}\right)+\frac{da}{dx}\left(2\frac{a^3}{s^3}\right)\right]+2\alpha s\frac{da}{dx}\left[2\left(1-\frac{a^2}{s^2}\right)-\frac{s}{a}\left(1+\frac{a^2}{s^2}\right)^2\sin^{-1}\frac{2\frac{a}{s}}{1+\frac{a^2}{s^2}}\right] \quad (16)$$

The lift and pitching-moment coefficients may now be determined by integration of the forces on all the elemental strips

$$C_L=\frac{1}{S_H}\int\frac{d}{dx}\left(\frac{L}{q}\right)dx \quad (17)$$

$$C_m=-\frac{1}{S_Hc_H}\int x\frac{d}{dx}\left(\frac{L}{q}\right)dx \quad (18)$$

where the integration interval extends from the most forward to the most rearward part of the wing-body combination.

PLANE-WING AND BODY COMBINATIONS

APPLICATIONS

For a given wing-body combination complying with the general requirements of the present theory, the load distribution may be determined directly by substituting the proper values for the body radius and wing semispan and their rate of change with x into equations (11) and (12). In addition, closed expressions for the lift, pitching moment, and center-of-pressure position of several elementary configurations may readily be found by simple integration of the integrals indicated by equations (13), (14), and (15). Several such applications will be presented in detail in this section and the results will be compared with those from other theories when possible.

Pointed low-aspect-ratio wing.—Although the assumptions of this note have been used previously by R. T. Jones in reference 8 to determine the aerodynamic properties of low-aspect-ratio wings, the load distribution, lift, and pitching moment will be rederived for completeness of presentation and to show a simple application of the preceding expressions. The aerodynamic properties of a low-aspect-ratio wing without fuselage may be determined by letting

$$\frac{a}{s}=0;\qquad\frac{da}{dx}=0$$

By substitution of these values into equation (11), it follows that the load distribution along any elemental spanwise strip is

$$\left(\frac{\Delta p_L}{q}\right)_H=\frac{4\alpha\frac{ds}{dx}}{\sqrt{1-\frac{y^2}{s^2}}} \quad (19)$$

The loading thus shows an infinite peak along the leading edge of the wing. The total load on an elemental spanwise strip is found from equation (16) to be

$$\frac{d}{dx}\left(\frac{L}{q}\right)q=4\pi\alpha q s\frac{ds}{dx} \tag{20}$$

Equations (19) and (20) show that the development of lift by the long slender wing depends on an expansion of the sections in a downstream direction. Accordingly, a part of the wing having parallel sides would develop no lift; whereas a part having contracting width would have negative lift with infinite negative loads along the edges. In the actual flow, however, no such loads can exist on the trailing edge. Further, it can be shown, by consideration of the Kutta condition and of the fact that the portion of the wing behind the station of maximum span lies completely within the vortex sheet trailing from the surface ahead, that the downwash field of these vortices is just such that the flow is directed parallel to the wing surface at all points behind the station of maximum span. Therefore, it can be concluded that the differential pressure acting on all such points is zero. This is known to be an oversimplification of the truth in the case of wings of nonvanishing aspect ratio at other than sonic speeds and caution should be exercised in applying the present results (particularly the pressure-distribution results) in regions of constant or contrating width.

The lift coefficient for this wing is found by integration of the load on the elemental strips between the leading edge and the widest section as indicated by substituting equation (20) into equation (17)

$$C_{L_W}=\frac{1}{S_H}\int_0^{c'_H}4\pi\alpha s\frac{ds}{dx}dx=\frac{4\pi\alpha}{S_H}\int_0^{s_0}sds=\frac{\pi}{2}\alpha\frac{4s_0^2}{S_H}=\frac{\pi}{2}A_H\alpha \tag{21}$$

Where c'_H is the effective wing chord and $\frac{4s_0^2}{S_H}=A_H$ the aspect ratio. It is seen that the lift-curve slope $\frac{dC_{L_W}}{d\alpha}$ depends only on the aspect rato. It should be noted, however, that the actual lift force depends only on the span and angle of attack and not on the aspect ratio or the area.

By similar substitution and integration by parts of equation (18), the pitching moment about the leading apex is

$$C_{m_W}=-\frac{1}{S_Hc_H}\int_0^{c'_H}4\pi\alpha s\frac{ds}{dx}x\,dx=-\frac{\pi}{2}\frac{c'_H}{c_H}\alpha\left(\frac{4s_0^2}{S_H}-\frac{4s_m^2}{S_H}\right)$$

$$=-\frac{\pi}{2}\frac{c'_H}{c_H}A_H\alpha\left(1-\frac{s_m^2}{s_0^2}\right) \tag{22}$$

where

$$s_m^2=\frac{1}{c'_H}\int_0^{c'_H}s^2dx$$

and where moments tending to produce a nosing-up rotation are considered positive. The center-of-pressure location is then found by dividing the moment coefficient by the lift coefficient as indicated in equation (15),

$$\frac{x_{c.p.}}{c_H}=-\frac{C_{m_H}}{C_{L_H}}=\frac{c'_H}{c_H}\left(1-\frac{4s_m^2}{S_HA_H}\right)=\frac{c'_H}{c_H}\left(1-\frac{s_m^2}{s_0^2}\right) \tag{23}$$

For a more specific example, consider a triangular wing moving point foremost. Then, since $s_m^2=\frac{1}{3}s_0^2$ and $c'_H=c_H$, the pitching-moment coefficient and center-of-pressure position are given, respectively, by $C_{m_W}=-\frac{\pi}{3}A_H\alpha$ and $\frac{x_{c.p.}}{c_H}=\frac{2}{3}$. The center of pressure is seen to be at the two-thirds chord point or the center of area.

To provide further insight into the range of applicability of the present theory, figure 3 has been prepared illustrating the variation of lift-curve slope with Mach number as predicted by the present theory (solid lines) and by linearized lifting-surface theory based on equation (1) (dotted lines).

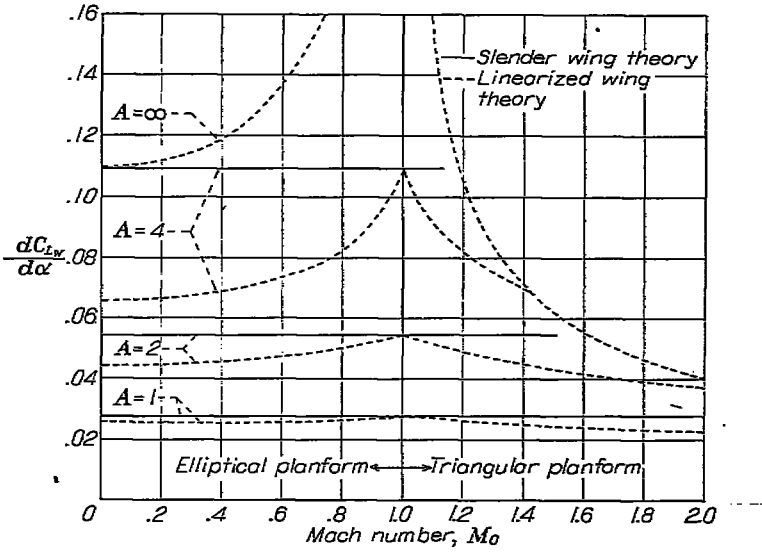

FIGURE 3.—Variation of lift-curve slope with Mach number.

In the subsonic range, the dotted curves are for wings of elliptical plan form and are based on Krienes' lifting-surface theory (reference 12) as modified for the effect of compressibility by Robinson and Young (reference 13), using the three-dimensional Prandtl-Glauert rule. For the supersonic case, the dotted curves are for wings of triangular plan form and are based on the theories of Robinson, Stewart, Brown, and others (references 14, 15, and 16). The solid curves representing the results of the present theory are valid for both elliptic and triangular wings; in fact, they are valid for any plan form such that no part of the trailing edge extends forward of the station of maximum span. It is clearly seen that for wings of low aspect ratio, the present theory agrees very well with the prediction of linearized lifting-surface theory at all Mach numbers; whereas for wings of larger aspect ratio the agreement is only satisfactory at Mach numbers near 1. This latter observation is very important for these wings if the aspect ratio is less than perhaps 3 or 4. For wings of higher aspect ratio, however, the agreement is probably only of academic interest since it is a well-known fact that experiment and linearized theory are in poor agreement for high-aspect-ratio wings at Mach numbers near unity. If comparable information were available for wing-body combinations, it is presumed that the results of the present theory would bear a similar relationship to the results of linearized theory.

Pointed slender body of revolution.—The present method for treating the flow around long slender bodies was introduced by Munk in reference 7 for the determination of the distribution of forces along the longitudinal axis of a body of revolution (airship hull). In the present section, these results will be rederived and, in addition, expressions for the total lift, pitching moment, and load distribution will be presented.

For the slender pointed body of revolution, the following relations exist:

$$\frac{a}{s}=1; \qquad \frac{da}{dx}=\frac{ds}{dx}$$

where $\frac{da}{dx}$ is not necessarily constant. If these values are substituted into equation (12), the load distribution along any elemental strip is

$$\left(\frac{\Delta p_L}{q}\right)_B=8\alpha\frac{da}{dx}\sin\theta=8\alpha\frac{da}{dx}\sqrt{1-\frac{y^2}{a^2}} \tag{24}$$

The load distribution on any strip is thus seen to be elliptical, being zero at the extremities of a horizontal diameter and a maximum at the midpoint. The total load on an elemental spanwise strip is found from equation (16) to be

$$\frac{d}{dx}\left(\frac{L}{q}\right)q=4\pi\alpha qa\frac{da}{dx}=2\alpha q\frac{dB}{dx} \tag{25}$$

where B is the local cross-section area. It is seen that equation (25) is identical to equation (20) for the integrated load on an elemental spanwise strip of a triangular wing, even though the distribution of load in the two cases is widely different. However, in contrast to equation (20), which is to be applied only to wings of increasing span, equation (25) may be applied to bodies of revolution in regions of either increasing or decreasing radius, since the Kutta condition does not apply to bodies of revolution. Thus, in general, the lift and pitching moment of a body of revolution are different from those of a wing of identical plan form; however, if the maximum diameter of the body of revolution is at the base station, its lift and pitching moment are equal to those of a wing of identical plan form at the same angle of attack.

As before, the lift coefficient will be determined by substituting equation (25) into equation (17). Taking the area of the base cross section B_b as the reference area and integrating over the length of the body l, the lift coefficient is found to be

$$C_L=\frac{1}{B_b}\int_0^l 2\alpha\frac{dB}{dx}\,dx=2\alpha \tag{26}$$

since the cross-section area B is B_b at $x=l$ and zero at $x=0$. It is thus seen that the lift of a slender body of revolution depends only on the cross-section area of the base, and is independent of the general shape of the body.

Such a relationship is indicative of an effect that would result from the inclusion of viscosity in the analysis, since the effective base area of the body will be larger than the true base area by an amount dependent on the boundary-layer thickness. Therefore, equation (26) will tend to underestimate the true lift-curve slope, particularly at lower Reynolds numbers where the boundary-layer thickness is greatest.

By similar substitution and integration by parts, the pitching-moment coefficient about the leading apex is

$$C_m=-\frac{1}{B_b l}\int_0^l 2\alpha\frac{dB}{dx}x\,dx=-2\alpha\left(1-\frac{B_m}{B_b}\right) \tag{27}$$

where B_m is the mean cross-section area (i. e., the volume of the body divided by the length). The center-of-pressure location is then found through use of equation (15) to be

$$\frac{x_{c.p.}}{l}=-\frac{C_m}{C_L}=1-\frac{B_m}{B_b} \tag{28}$$

For a more specific example, consider a cone moving point foremost. The base cross-section area is

$$B_b=\pi a_0^2$$

The mean cross-section area is

$$B_m=\frac{1}{3}\pi a_0^2$$

The center of pressure is thus seen to be at the two-thirds point as would be anticipated by the conical nature of the load distribution for this case.

Triangular wing with conical body.—The first example of a wing-body combination to be considered is that of a conical body mounted on a triangular wing so that their vertices coincide. The geometry of such a configuration requires that

$$\frac{a}{s}=\frac{da/dx}{ds/dx}=K_H$$

where both da/dx and ds/dx are constants. If these values are substituted into equations (11) and (12) as described in the two preceding examples, the load distribution along any elemental strip of the wing is given by

$$\left(\frac{\Delta p_L}{q}\right)_H=4\alpha\frac{ds}{dx}\left[\frac{1+K_H{}^4-2K_H{}^4\frac{s^2}{y^2}}{\sqrt{1+K_H{}^4-\frac{y^2}{s^2}\left(1+K_H{}^4\frac{s^4}{y^4}\right)}}\right] \tag{29}$$

and on the body by

$$\left(\frac{\Delta p_L}{q}\right)_B=4\alpha\frac{ds}{dx}\sqrt{(1+K_H{}^2)^2-4\frac{y^2}{s^2}} \tag{30}$$

The integrated load on an elemental strip is

$$\frac{d}{dx}\left(\frac{L}{q}\right)q=4\pi\alpha qs\frac{ds}{dx}\left\{1+K_H{}^4+\frac{1}{2\pi}\left[2K_H(1-K_H{}^2)-(1+K_H{}^2)^2\sin^{-1}\frac{2K_H}{1+K_H{}^2}\right]\right\}=4\pi\alpha qs\frac{ds}{dx}\sigma_H \tag{31}$$

where

$$\sigma_H=1+K_H{}^4+\frac{1}{2\pi}\left[2K_H(1-K_H{}^2)-(1+K_H{}^2)^2\sin^{-1}\frac{2K_H}{1+K_H{}^2}\right]$$

The lift coefficient for the entire conical wing-body combination is then

$$C_L=\frac{\pi}{2}A_H\alpha\,\sigma_H=C_{L_W}\sigma_H \tag{32}$$

where C_{L_W} is the lift coefficient of the basic triangular wing. Due to the radial nature of the lines of constant pressure, the center of pressure lies at the two-thirds chord point

$$\frac{x_{c.p.}}{c_H}=\frac{2}{3} \tag{33}$$

The moment coefficient is then obviously

$$C_m=-\frac{\pi}{3}A_H\alpha\,\sigma_H=C_{m_W}\sigma_H \tag{34}$$

where, as before, C_{m_W} represents the pitching moment of the basic wing. In equations (32) and (34), the reference area, aspect ratio, and chord of the wing-body combination are considered to be the same as those of the basic wing.

Figures 4 and 5 show, respectively, the lift and pitching-moment results. It may be seen that, although the wing

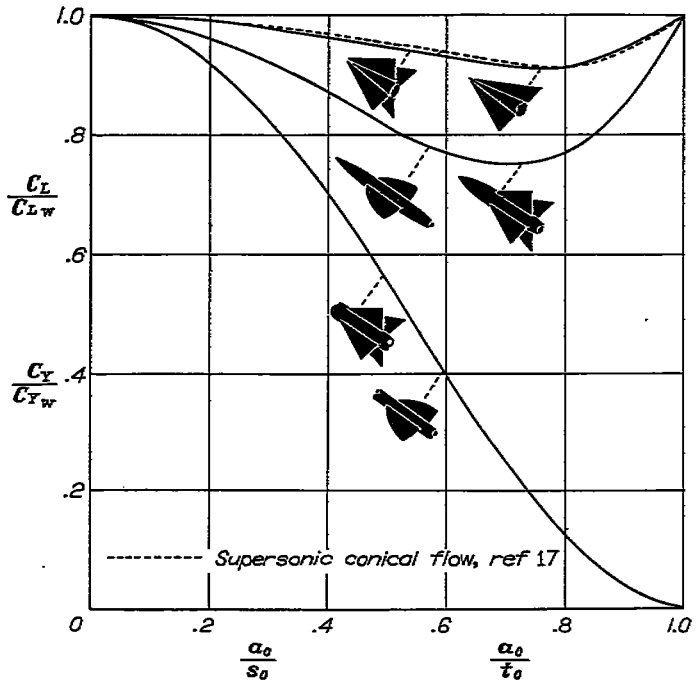

FIGURE 4.—Lift and side-force ratios for several wing-body combinations.

alone and body alone have identical lift- and moment-curve slopes since the widest section is at the trailing edge, the lift- and moment-curve slopes of the wing-body combination are always less than those of either the wing or the body alone.

Also shown in figure 4 is a curve presented by Browne, Friedman, and Hodes (reference 17) for the lift-curve slope, as calculated by means of conventional linearized theory, of a wing-body combination consisting of a conical body having a fixed radius of 0.1322 the Mach cone radius and a triangular wing of varying span. This curve never deviates from that given by the present theory by as much as 1 percent.

Low-aspect-ratio wing on an infinite cylindrical body.—The next example to be considered is that of a low-aspect-ratio

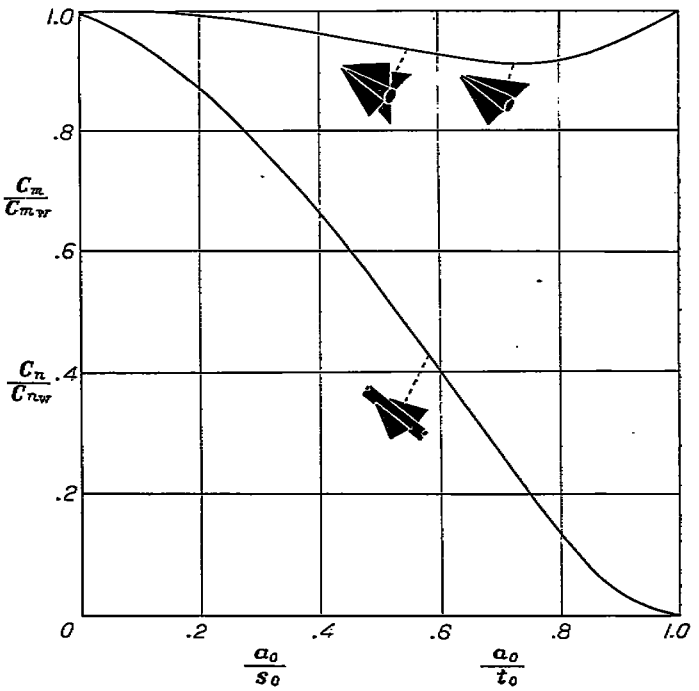

FIGURE 5.—Pitching-moment and yawing-moment ratios for several wing-body combinations.

wing mounted on an infinite cylindrical body. Except for the requirement that no part of the trailing edge may lie forward of the station of maximum span, the wing plan form is arbitrary. The essential relationships to be used are that

$$a=a_0; \qquad \frac{da}{dx}=0$$

and that ds/dx is a positive quantity. By using these relationships as in the previous examples, it is found that no lift is carried on the body ahead of the leading edge of the root chord. Further, as in the case of the wing alone, no lift is carried on either the wing or on the body aft of the stations of maximum wing span. Between these stations, however, lift is carried on both the wing and body and is distributed on any elemental strip of the wing in a manner described by

$$\left(\frac{\Delta p_L}{q}\right)_H=\frac{4\alpha\frac{ds}{dx}\left(1-\frac{a_0^4}{s^4}\right)}{\sqrt{\left(1+\frac{a_0^4}{s^4}\right)-\frac{y^2}{s^2}\left(1+\frac{a_0^4}{y^4}\right)}} \tag{35}$$

and on the body by

$$\left(\frac{\Delta p_L}{q}\right)_B=\frac{4\alpha\frac{ds}{dx}\left(1-\frac{a_0^4}{s^4}\right)}{\sqrt{\left(1+\frac{a_0^2}{s^2}\right)^2-4\frac{y^2}{s^2}}} \tag{36}$$

The integrated load on an elemental strip is given by

$$\frac{d}{dx}\left(\frac{L}{q}\right)q=4\pi\alpha qs\frac{ds}{dx}\left(1-\frac{a_0^4}{s^4}\right) \tag{37}$$

By integration along the length of the body, the lift coefficient for the complete wing-body combination is found to be

$$C_L=\frac{\pi}{2}A_H\alpha\left(1-\frac{a_0^2}{s_0^2}\right)^2=C_{L_W}\left(1-\frac{a_0^2}{s_0^2}\right)^2 \tag{38}$$

where C_L and C_{L_W} are both based on the same reference area. It may be seen from equation (38) and figure 4 that the addition of a cylindrical body to a low-aspect-ratio wing produces a loss in lift-curve slope just as in the preceding example with the conical body. With the cylindrical body, however, the lift-curve slope has no minimum value, but continues to decrease as the radius-semispan ratio increases until finally, when the latter ratio is one (corresponding to a body without wings), the lift-curve slope is zero. This is as it should be, since an infinite cylindrical body has zero lift-curve slope in an ideal nonviscuous fluid. The moment coefficient about the leading edge of the root chord is

$$C_m=-\frac{\pi A_H\alpha}{2}\frac{c'_H}{c_H}\left[\left(1+\frac{a_0^4}{s_0^4}\right)-\int_0^1\left(\frac{s}{s_0}\right)^2 d\left(\frac{x}{c'_H}\right)-\frac{a_0^4}{s_0^4}\int_0^1\frac{d(x/c'_H)}{(s/s_0)^2}\right] \tag{39}$$

For a more specific example, consider the case where the leading edge of the wing extends in a straight line from the body to the point of maximum span. The shape of the trailing edge is arbitrary, except for the requirement that no part of the trailing edge may lie forward of the station of maximum span. The pitching-moment coefficient about the leading edge of the root chord is then

$$\begin{aligned}C_m&=-\frac{\pi A_H\alpha}{6}\frac{c'_H}{c_H}\left[\left(1-\frac{a_0}{s_0}\right)^2\left(2+3\frac{a_0}{s_0}+3\frac{a_0^2}{s_0^2}\right)\right]\\&=\frac{1}{2}C_{m_W}\left[\left(1-\frac{a_0}{s_0}\right)^2\left(2+3\frac{a_0}{s_0}+3\frac{a_0^2}{s_0^2}\right)\right]\end{aligned} \tag{40}$$

where c_H represents the root chord of the wing and c'_H represents the effective chord, that is, the longitudinal distance between the leading edge of the root chord and the station of maximum span. If each half-wing is a triangle, the ratio of the pitching moment of the wing-body combination to that of the wing alone for various body radii to wing semispan ratios may be represented by a single curve, since the effective chord ratio c'_H/c_H is a constant. This curve is shown in figure 5. If the complete wing is a triangle (or each half-wing is a right triangle), the effective chord ratio is, of course, unity. If figure 5 is used, or the latter form of equation (40), it should be remembered that C_m represents the pitching moment about the leading edge of the root chord and is nondimensionalized using the root chord as a reference length.

It is important to note that the ratio of the lift of a wing-body combination having a low-aspect-ratio wing and an infinite cylindrical body to that of the wing alone given by equation (38) can be shown directly by momentum-theory considerations to apply to any wing-body combination comprised of an infinite cylindrical body and a completely arbitrary wing and traveling at either subsonic or supersonic speed, provided the span loading is that corresponding to minimum vortex drag. This conclusion, in a more restricted sense, has been given previously by Lennertz (see reference 18, p. 276) for the incompressible flow about wing-body combinations composed of an infinite cylinder and a lifting line.

Low-aspect-ratio wing on a pointed body.—The case of a low-aspect-ratio wing mounted on a pointed body, closed in an arbitrary manner at the nose, cylindrical along the wing-root chord, and either cylindrical or tapered behind the wing, may be studied by combining the results of two previous examples. The portion of the wing-body combination ahead of the leading edge of the wing root may be considered to be equivalent to the arbitrary body of revolution treated in the second example. The portion of the wing-body combination at stations along the wing root is equivalent to a low-aspect-ratio wing mounted on an infinite cylinder as discussed in the preceding example. The forces exerted on the portion of the body aft of the wing will be considered to be zero. As can be shown by the extension of slender-body theory to cases involving curving air streams given in reference 5, this conclusion is only strictly true if the portion of the body aft of the wing is cylindrical or is tapered to a point. For intermediate cases, however, the forces are always very small quantities and can be taken, for the present problem, to be sensibly zero. The load distribution and the integrated load on any elemental spanwise strip are then the same as those given in the corresponding examples.

The lift coefficient is found by adding the lift forces of the component parts of the wing-body combination and dividing by the dynamic pressure q and the characteristic area. The lift coefficient is then found to be

$$C_L=\frac{\pi}{2}A_H\alpha\left(1-\frac{a_0^2}{s_0^2}+\frac{a_0^4}{s_0^4}\right) \tag{41}$$

Figure 4 shows the variation of the lift-curve slope with body-radius wing-semispan ratio. A comparison of the lift-curve slopes shows that the loss in the lift of a wing resulting from the addition of a body having a pointed nose is much less than that resulting from the addition of an infinite body.

The moment coefficient for this wing-body combination may be found in a manner similar to that used in finding the lift coefficient, taking care to transfer the moments of both component parts to the same axis. The moment coefficient about the leading edge of the root chord is

$$C_m=-\frac{\pi A_H\alpha}{6}\frac{c'_H}{c_H}\left[\left(1-\frac{a_0}{s_0}\right)^2\left(2+3\frac{a_0}{s_0}+\frac{a_0^2}{s_0^2}\right)\right]+2\alpha\frac{B_m}{S_H}\frac{l}{c_H} \tag{42}$$

where l and B_m represent, respectively, the length and mean cross-sectional area (i. e., volume divided by length) of the portion of the body ahead of the leading edge of the wing root and a_0 represents the radius of the cylindrical portion of the body.

CRUCIFORM-WING AND BODY COMBINATIONS

THEORY

The foregoing theory may be extended to enable the prediction of the load distribution and aerodynamic properties of slender cruciform-wing and body combinations inclined at small angles of pitch α and yaw β. (See fig. 6.) As in the preceding case, the wing-body combination is considered to consist of a slender body of revolution and flat highly swept-back, low-aspect-ratio wings. The wings, designated horizontal and vertical, extend along the continuation of the horizontal and vertical meridian planes of the body. These

problems may be treated by determining the perturbation velocity potenial ϕ by means of equation (2) together with the following boundary conditions: at the surface of the horizontal wing

$$\frac{\partial\phi}{\partial z}=0 \tag{43}$$

at the surface of the vertical wing

$$\frac{\partial\phi}{\partial y}=0 \tag{44}$$

at the surface of the body

$$\frac{\partial\phi}{\partial r}=0 \tag{45}$$

infinitely far ahead or to the side of the wing-body combination

$$\text{grad } \phi=\bar{k}V_0\alpha-\bar{j}V_0\beta \tag{46}$$

where $\bar{j}$ and $\bar{k}$ are unit vectors in the y and z directions, respectively, and finally ϕ is continuous everywhere except across the surface of the wing-body combination or its wake.

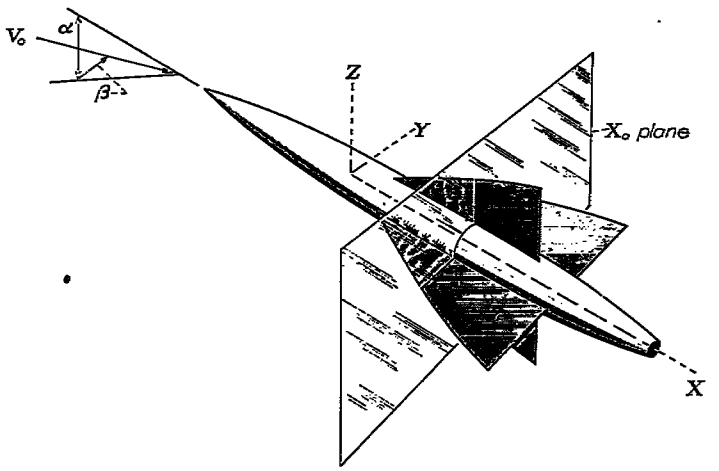

FIGURE 6.—View of cruciform-wing and body combination showing coordinate axes.

Velocity potential.—As in the case of plane-wing and body combinations, the perturbation velocity field in the x_0 plane is similar to the velocity field around an infinitely long cylinder, the cross section of which corresponds to the trace of the wing-body combination in the x_0 plane. For a slender cruciform-wing and body combination inclined an angle α in pitch and β in yaw, the flow in the x_0 plane is as shown in figure 7 (a) where the component of the flow velocity at infinity in the z direction is $V_0\alpha$ and that in the y direction is $-V_0\beta$. The flow field of figure 7 (a) can obviously be considered to be the sum of the two flow fields shown in figures 7 (b) and 7 (c), since the vertical wing in figure 7 (b) and the horizontal wing in figure 7 (c) lie in planes of symmetry and cannot affect the flow shown in their respective figures. Thus, the flow fields shown in figures 7 (b) and 7 (c) are identical to those of figures 7 (d) and 7 (e), respectively. The velocity potential for such a flow field was derived in the preceding section from the flow field about a straight line (fig. 7 (f)). The expression for the velocity potential of the flow field shown in figure 7 (b) is thus identical to that given in equation (9) for the flow field of figure 2 (a)

$$\phi_a=\pm\frac{V_0\alpha}{\sqrt{2}}\left\{\left[-\left(1+\frac{a^4}{r^4}\right)r^2\cos 2\theta+s^2\left(1+\frac{a^4}{s^4}\right)\right]+\left[r^4\left(1-\frac{a^4}{r^4}\right)^2+4a^4\cos^2 2\theta+s^4\left(1+\frac{a^4}{s^4}\right)^2-2s^2\left(1+\frac{a^4}{r^4}\right)\left(1+\frac{a^4}{s^4}\right)r^2\cos 2\theta\right]^{1/2}\right\}^{1/2} \tag{47a}$$

where the sign is positive in the upper half plane ($0<\theta<\pi$) and negative in the lower half plane $\pi<\theta<2\pi$. The expression for the velocity potential for the flow field shown in figure 7 (c) is found in a similar manner to be

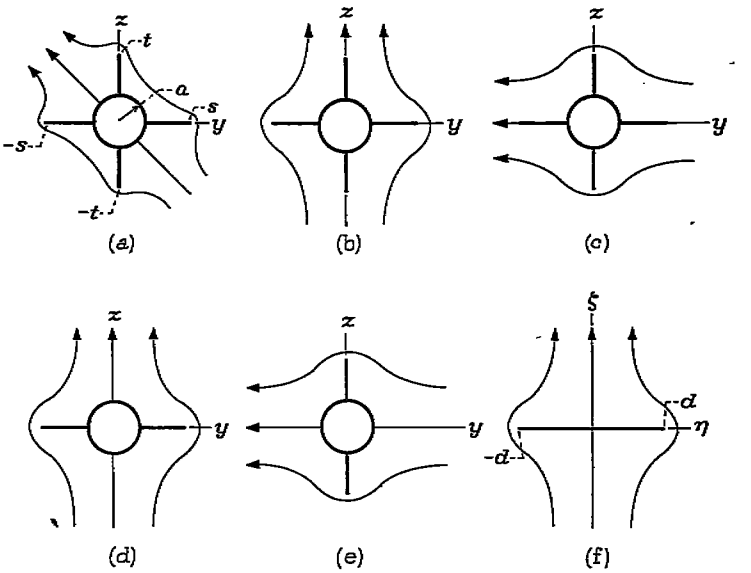

FIGURE 7.—Two-dimensional flow fields corresponding to cruciform-wing and body combinations.

$$\phi_b=\pm\frac{V_0\beta}{\sqrt{2}}\left\{\left[\left(1+\frac{a^4}{r^4}\right)r^2\cos 2\theta+t^2\left(1+\frac{a^4}{t^4}\right)\right]+\left[r^4\left(1-\frac{a^4}{r^4}\right)^2+4a^4\cos^2 2\theta+t^4\left(1+\frac{a^4}{t^4}\right)^2+2t^2\left(1+\frac{a^4}{t^4}\right)\left(1+\frac{a^4}{r^4}\right)r^2\cos 2\theta\right]^{1/2}\right\}^{1/2} \tag{47b}$$

where the sign is positive in the left half plane ($\pi/2<\theta<3\pi/2$) and negative in the right half plane ($-\pi/2<\theta<\pi/2$). The perturbation velocity potential for the flow field about a cruciform-wing and body combination inclined in both pitch and yaw is then given by

$$\phi=\phi_a+\phi_b \tag{47c}$$

Load distribution.—As shown in equation (10), the differential pressure coefficient between any two points in linearized potential flow is given by

$$\frac{\Delta p}{q}=\frac{2\Delta u}{V_0} \tag{48}$$

where Δu is the difference of the components in the free-stream direction of the perturbation velocities at the two

points. Since body axes are used in the present treatment rather than wind axes, the component of Δu in the free-stream direction will be approximated to first-order terms. The differential pressure coefficient is then given by

$$\frac{\Delta p}{q}=\frac{2}{V_0}\left(\Delta\frac{\partial\phi}{\partial x}-\beta\Delta\frac{\partial\phi}{\partial y}+\alpha\Delta\frac{\partial\phi}{\partial z}\right) \tag{49}$$

The last two terms of equation (49) are often omitted, since they each represent the product of a small angle and a small perturbation velocity and are generally much smaller than the first term on the right-hand side, which represents only a perturbation velocity. For the long slender wings, bodies, and wing-body combinations considered here, however, $\partial\phi/\partial x$ is much smaller than $\partial\phi/\partial y$ and $\partial\phi/\partial z$; therefore, all three terms are retained. The last term of the right-hand member of equation (49) was not included in the corresponding equation (equation (10)) for plane-wing and body combinations inclined only in pitch since, for that case, it is zero by reason of symmetry.

Through application of equations (47) and (49), expressions for the lifting differential pressure (lower minus upper) on the horizontal wing and body are found to be, respectively,

$$\left(\frac{\Delta p_L}{q}\right)_H=4\alpha\left\{\frac{\left[\frac{ds}{dx}\left(1-\frac{a^4}{s^4}\right)+2\frac{a}{s}\frac{da}{dx}\left(\frac{a^2}{s^2}-\frac{a^2}{y^2}\right)\right]+\left[\beta\frac{y}{s}\left(1-\frac{a^4}{y^4}\right)\right]}{\sqrt{\left(1+\frac{a^4}{s^4}\right)-\frac{y^2}{s^2}\left(1+\frac{a^4}{y^4}\right)}}\right\} \tag{50}$$

$$\left(\frac{\Delta p_L}{q}\right)_B=4\alpha\left\{\frac{\left[\frac{ds}{dx}\left(1-\frac{a^4}{s^4}\right)+2\frac{a}{s}\frac{da}{dx}\left(\frac{a^2}{s^2}+1-\frac{2y^2}{a^2}\right)\right]+\left[4\beta\frac{y}{s}\left(1-\frac{y^2}{a^2}\right)\right]}{\sqrt{\left(1+\frac{a^2}{s^2}\right)^2-4\frac{y^2}{s^2}}}\right\}\pm\frac{16\alpha\beta\left(\frac{y^2}{at}\right)\sqrt{1-\frac{y^2}{a^2}}}{\sqrt{\left(1-\frac{a^2}{t^2}\right)^2+4\frac{y^2}{t^2}}} \tag{51}$$

where, in equation (51), the plus sign is taken for the starboard side of the body and the minus sign for the port side. Similarly, the yawing differential pressure (port minus starboard) on the vertical wing and body are given, respectively, by

$$\left(\frac{\Delta p_Y}{q}\right)_V=4\beta\left\{\frac{-\left[\frac{dt}{dx}\left(1-\frac{a^4}{t^4}\right)+2\frac{a}{t}\frac{da}{dx}\left(\frac{a^2}{t^2}-\frac{a^2}{z^2}\right)\right]+\left[\alpha\frac{z}{t}\left(1-\frac{a^4}{z^4}\right)\right]}{\sqrt{\left(1+\frac{a^4}{t^4}\right)-\frac{z^2}{t^2}\left(1+\frac{a^4}{z^4}\right)}}\right\} \tag{52}$$

$$\left(\frac{\Delta p_Y}{q}\right)_B=4\beta\left\{\frac{-\left[\frac{dt}{dx}\left(1-\frac{a^4}{t^4}\right)+2\frac{a}{t}\frac{da}{dx}\left(\frac{a^2}{t^2}+1-2\frac{z^2}{a^2}\right)\right]+\left[4\alpha\frac{z}{t}\left(1-\frac{z^2}{a^2}\right)\right]}{\sqrt{\left(1+\frac{a^2}{t^2}\right)^2-4\frac{z^2}{t^2}}}\right\}\pm\frac{16\alpha\beta\left(\frac{z^2}{as}\right)\sqrt{1-\frac{z^2}{a^2}}}{\sqrt{\left(1-\frac{a^2}{s^2}\right)^2+4\frac{z^2}{s^2}}} \tag{53}$$

where, in equation (53), the plus sign is taken for the upper side of the body and the minus sign for the lower side. As was pointed out for plane-wing and body combinations, the expressions for the pressures on the body are not applicable at stations behind the trailing edge of the wing. From the same arguments as advanced before, the forces on this portion of the body will be taken to be zero.

Total forces and moments.—The total forces and moments exerted on a complete cruciform-wing and body combination may be determined by integrating the loading over the entire surface area. As with plane-wing and body combinations, it is convenient to carry out the integration by first evaluating the forces and moments on one transverse strip, and then integrating these elemental quantities over the length of the wing-body combination. The lift and side force on a transverse strip of width dx are given, respectively, by

$$dL=qdx\int_{-s}^{+s}\left(\frac{\Delta p_L}{q}\right)dy \tag{54}$$

$$dY=qdx\int_{-t}^{+t}\left(\frac{\Delta p_Y}{q}\right)dz \tag{55}$$

The rolling moment on this elemental strip is given by

$$dL'=qdx\left[-\int_{-s}^{-a}y\left(\frac{\Delta p_L}{q}\right)_H dy-\int_a^s y\left(\frac{\Delta p_L}{q}\right)_H dy+\int_{-t}^{-a}z\left(\frac{\Delta p_Y}{q}\right)_V dz+\int_a^t z\left(\frac{\Delta p_Y}{q}\right)dz\right] \tag{56}$$

where the integration is carried only over the surface of the wing, since pressures on the body cannot produce a rolling moment. When the indicated operations are performed, the following expressions for the elemental lift, side force, and rolling moment are obtained:

$$\frac{d}{dx}\left(\frac{L}{q}\right)=4\pi\alpha s\left[\frac{ds}{dx}\left(1-\frac{a^4}{s^4}\right)+\frac{da}{dx}\left(2\frac{a^3}{s^3}\right)\right]+2\alpha s\frac{da}{dx}\left[2\left(1-\frac{a^2}{s^2}\right)-\frac{s}{a}\left(1+\frac{a^2}{s^2}\right)\sin^{-1}\frac{2as}{s^2+a^2}\right] \tag{57}$$

$$\frac{d}{dx}\left(\frac{Y}{q}\right)=-4\pi\beta t\left[\frac{dt}{dx}\left(1-\frac{a^4}{t^4}\right)+\frac{da}{dx}\left(2\frac{a^3}{t^3}\right)\right]-2\beta t\frac{da}{dx}\left[2\left(1-\frac{a^2}{t^2}\right)-\frac{t}{a}\left(1+\frac{a^2}{t^2}\right)^2\sin^{-1}\frac{2at}{t^2+a^2}\right] \tag{58}$$

$$\frac{d}{dx}\left(\frac{L'}{q}\right)=2\alpha\beta t^2\left[2\frac{a}{t}\left(1-\frac{a^2}{t^2}\right)+\pi\left(1+\frac{a^4}{t^4}\right)-\left(1+\frac{a^2}{t^2}\right)^2\cos^{-1}\frac{t^2-a^2}{t^2+a^2}\right]-2\alpha\beta s^2\left[2\frac{a}{s}\left(1-\frac{a^2}{s^2}\right)+\pi\left(1+\frac{a^4}{s^4}\right)-\left(1+\frac{a^2}{s^2}\right)^2\cos^{-1}\frac{s^2-a^2}{s^2+a^2}\right] \tag{59}$$

The forces and moments for the complete wing-body combination may now be determined by integration of the forces on all the elemental strips. Expressed in nondimensional form, these characteristics are given by

$$C_L=\frac{1}{S_H}\int\frac{d}{dx}\left(\frac{L}{q}\right)dx \tag{60}$$

$$C_m=-\frac{1}{S_Hc_H}\int\frac{d}{dx}\left(\frac{L}{q}\right)x\,dx \tag{61}$$

$$C_Y=\frac{1}{S_V}\int\frac{d}{dx}\left(\frac{Y}{q}\right)dx \tag{62}$$

$$C_n=-\frac{1}{S_Vc_V}\int\frac{d}{dx}\left(\frac{Y}{q}\right)x\,dx \tag{63}$$

$$C_l=\frac{1}{2s_0S_H}\int\frac{d}{dx}\left(\frac{L'}{q}\right)dx \tag{64}$$

where the integration interval extends from the most forward to the most rearward part of the wing-body combination. To achieve a unity of expression for side force and lift and for yawing moment and pitching moment, the side-force coefficients have been based upon the area of the vertical wing rather than the more conventional horizontal-wing area, and the yawing-moment coefficients have been based upon the area and root chord of the vertical wing rather than the area and span of the horizontal wing.

The expressions for the forces and moments on the elemental strips (equations (57), (58), and (59)) indicate four important general characteristics of slender cruciform-wing and body combinations. First of all, there is a complete correspondence of the expressions for the lift and side force as would be expected from the geometry of the configuration. Second, the lift is independent of the angle of yaw and the side force is independent of the angle of attack. Third, the expressions for the lift and pitching moment for slender cruciform-wing and body combinations are identical to those for plane-wing and body combinations. Last, if the vertical and horizontal wings are identical, the rolling moment is zero.

SLENDER CRUCIFORM-WING AND BODY COMBINATIONS

APPLICATIONS

The general expressions developed for slender cruciform-wing and body combinations will now be applied to several particular configurations. The discussion will be brief since the results are similar in many ways to those given for plane-wing and body combinations.

Pointed low-aspect-ratio wings, no body.—The first and simplest example of a slender cruciform configuration to be considered consists of a set of pointed low-aspect-ratio wings, which may have different plan forms and aspect ratios, and no body. The aerodynamic properties of such a configuration may be determined by letting

$$\frac{a}{s}=\frac{a}{t}=0;\qquad\frac{da}{dx}=0$$

By substitution of these values into equations (50) and (52), it follows that the load distributions for the horizontal and vertical wings are given by

$$\left.\begin{aligned}\left(\frac{\Delta p_L}{q}\right)_H&=\frac{4\alpha\left(\frac{da}{dx}+\beta\frac{y}{s}\right)}{\sqrt{1-\frac{y^2}{s^2}}}\\ \left(\frac{\Delta p_Y}{q}\right)_V&=-\frac{4\beta\left(-\frac{dt}{dx}+\alpha\frac{z}{t}\right)}{\sqrt{1-\frac{z^2}{t^2}}}\end{aligned}\right\} \tag{65}$$

These expressions are similar to that given by Ribner (reference 9) for the loading on a single low-aspect-ratio triangular wing inclined in pitch and yaw. The symmetric first terms contribute to lift and side force; the antisymmetric second terms contribute to rolling moments. To illustrate this point further, figure 8 has been prepared showing the load distribution on a cruciform arrangement of triangular wings. The loading on the vertical wing is shown by the two top sketches, while that on the horizontal wing is shown by the lower sketches. The sketches on the left represent the contribution of the symmetric first terms of equation (65); those on the right, the contribution of the antisymmetric second terms. In accordance with the stated assumptions, these expressions are invalid when either the angle of pitch or yaw becomes so large that the leading edge passes beyond the stream direction and becomes, effectively, a trailing edge. Mathematically expressed, the expressions are valid when $|\beta|\leq ds/dx$ and $|\alpha|\leq dt/dx$. If it is desired to investigate wings inclined at larger angles, consideration must be given to the influence of the trailing vortices lying outboard of one of the sides of the wing. Such a problem may be treated by an extension of the methods employed in the treatment of a swept-back wing in reference 10. The total load on an elemental strip is found from equations (57) and (58) to be

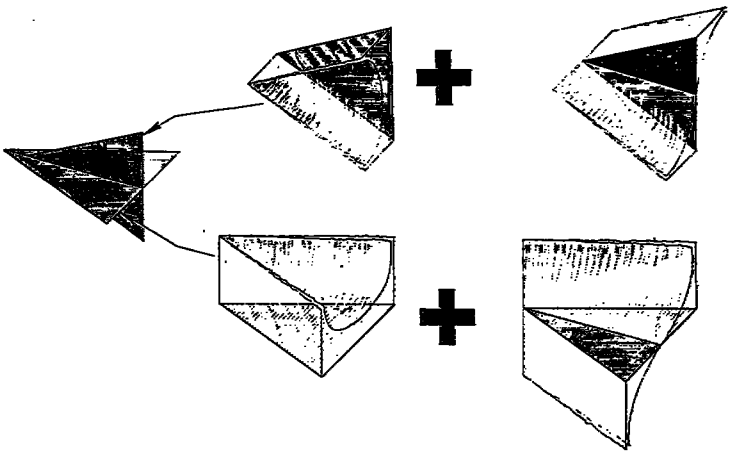

FIGURE 8.—Load distribution on a triangular cruciform wing.

$$\left.\begin{aligned}\frac{d}{dx}\left(\frac{L}{q}\right)q&=4\pi\alpha qs\frac{ds}{dx}\\ \frac{d}{dx}\left(\frac{Y}{q}\right)q&=-4\pi\beta qt\frac{dt}{dx}\end{aligned}\right\}\tag{66}$$

The rolling moments exerted on the horizontal and vertical wings are given, respectively, by the corresponding terms of equation (59)

$$\left.\begin{aligned}\frac{d}{dx}\left(\frac{L'}{q}\right)_H q&=-2\pi\alpha\beta qs^2\\ \frac{d}{dx}\left(\frac{L'}{q}\right)_V q&=2\pi\alpha\beta qt^2\end{aligned}\right\}\tag{67}$$

The lift and side-force coefficients for the cruciform wing are found by integration of the forces on the elemental strips between the leading apex and the trailing edge as indicated by substituting equation (66) into equations (60) and (62)

$$\left.\begin{aligned}C_{L_W}&=\frac{\pi}{2}A_H\alpha\\ C_{Y_W}&=-\frac{\pi}{2}A_V\beta\end{aligned}\right\}\tag{68}$$

where A_H and A_V are the aspect ratios of the horizontal and vertical wings, respectively.

Similarly, the pitching-, yawing-, and rolling-moment coefficients are found by substituting equations (66) and (67) into equations (61), (63), and (64), respectively, and integrating:

$$\left.\begin{aligned}C_{m_W}&=-\frac{\pi}{2}A_H\alpha\left(1-\frac{{s_m}^2}{{s_0}^2}\right)\\ C_{n_W}&=\frac{\pi}{2}A_V\beta\left(1-\frac{{t_m}^2}{{t_0}^2}\right)\end{aligned}\right\}\tag{69}$$

$$C_{l_W}=\frac{\pi\alpha\beta}{S_H s_0}(c_V{t_m}^2-c_H{s_m}^2)\tag{70}$$

where

$${s_m}^2=\frac{1}{c_H}\int_0^{c_H}s^2\,dx$$

$${t_m}^2=\frac{1}{c_V}\int_0^{c_V}t^2\,dx$$

Attention is called to the fact that the pitching- and yawing-moment coefficients represent moments about the leading apexes and are nondimensionalized through use of the area and root chord of the horizontal and vertical wings, respectively.

For a more specific example, consider the wings to be of triangular plan form moving point foremost. Then, since

$${s_m}^2=\frac{1}{3}{s_0}^2$$

and

$${t_m}^2=\frac{1}{3}{t_0}^2$$

the moment coefficients given by equations (69) and (70) are

$$\left.\begin{aligned}C_m&=-\frac{\pi}{3}A_H\alpha\\ C_n&=\frac{\pi}{3}A_V\beta\end{aligned}\right\}\tag{71}$$

$$C_l=\frac{\pi\alpha\beta}{3}\left(\frac{S_V t_0}{S_H s_0}-1\right)\tag{72}$$

Pointed slender body of revolution.—Expressions for the aerodynamic characteristics of a pointed slender body of revolution inclined in pitch and yaw may be derived from the previously derived equations by letting

$$\frac{a}{s}=1;\qquad \frac{da}{dx}=\frac{ds}{dx}=\frac{dt}{dx}$$

Since these results are essentially the same as given previously, only the final equations will be listed

$$\left(\frac{\Delta p_L}{q}\right)_B=8\alpha\frac{da}{dx}\sqrt{1-\frac{y^2}{a^2}};\qquad \left(\frac{\Delta p_Y}{q}\right)_B=-8\beta\frac{da}{dx}\sqrt{1-\frac{y^2}{a^2}}\tag{73}$$

$$\frac{d}{dx}\left(\frac{L}{q}\right)q=4\pi\alpha qa\frac{da}{dx}=2\alpha q\frac{dB}{dx};\qquad \frac{d}{dx}\left(\frac{Y}{q}\right)q=-2\beta q\frac{dB}{dx}\tag{74}$$

$$C_L=2\alpha\qquad C_Y=-2\beta\tag{75}$$

$$C_m=-2\alpha\left(1-\frac{B_m}{B_b}\right);\qquad C_n=2\beta\left(1-\frac{B_m}{B_b}\right)\tag{76}$$

where B is the local cross-section area, B_b is the area of the base, and B_m is the mean cross-section area (i. e., the volume of the body divided by the length). In the coefficients, the reference area is taken as the area of the base cross section.

Triangular cruciform wings with conical body.—The first example of a wing-body combination to be considered is a conical arrangement (coincident vertices) of a conical body and triangular vertical and horizontal wings of, in general, different aspect ratio. The geometry of such a configuration requres that

$$\frac{a}{s}=\frac{da/dx}{ds/dx}=K_H;\qquad \frac{a}{t}=\frac{da/dx}{dt/dx}=K_V$$

where da/dx, ds/dx, and dt/dx are constants. The load distribution along any elemental strip of the wings and body is given by

$$\left(\frac{\Delta p_L}{q}\right)_H=4\alpha\left[\frac{\frac{ds}{dx}\left(1+{K_H}^4-2{K_H}^4\frac{s^2}{y^2}\right)+\beta\frac{y}{s}\left(1-{K_H}^4\frac{s^4}{y^4}\right)}{\sqrt{(1+{K_H}^4)-\frac{y^2}{s^2}\left(1+{K_H}^4\frac{s^4}{y^4}\right)}}\right]$$

$$\left(\frac{\Delta p_L}{q}\right)_B=4\alpha\frac{ds}{dx}\sqrt{(1+{K_H}^2)^2-4{K_H}^2\left(\frac{y^2}{a^2}\right)}+$$

$$16\alpha\beta\left[\frac{K_H\left(\frac{y}{a}\right)\left(1-\frac{y^2}{a^2}\right)}{\sqrt{(1+{K_H}^2)^2-4{K_H}^2\left(\frac{y^2}{a^2}\right)}}\pm\right.$$

$$\frac{K_V\left(\frac{y^2}{a^2}\right)\sqrt{1-\frac{y^2}{a^2}}}{\sqrt{(1-K_V^2)^2+4K_V^2\frac{y^2}{a^2}}}\Bigg]$$

$$\left(\frac{\Delta p_V}{q}\right)_V=4\beta\left[\frac{-\frac{dt}{dx}\left(1+K_V^4-2K_V^4\left(\frac{t^2}{z^2}\right)+\alpha\frac{z}{t}\left(1-K_V^4\frac{t^4}{z^4}\right)\right.}{\sqrt{(1+K_V^4)-\frac{z^2}{t^2}\left(1+K_V^4\frac{t^4}{z^4}\right)}}\right]$$

$$\left(\frac{\Delta p_V}{q}\right)_B=-4\beta\frac{dt}{dx}\sqrt{(1+K_V^2)^2-4K_V^2\left(\frac{z^2}{a^2}\right)}+$$

$$16\alpha\beta\left[\frac{K_V\frac{z}{a}\left(1-\frac{z^2}{a^2}\right)}{\sqrt{(1+K_V^2)^2-4K_V^2\left(\frac{z^2}{a^2}\right)}}\pm\right.$$

$$\left.\frac{K_H\left(\frac{z^2}{a^2}\right)\sqrt{1-\frac{z^2}{a^2}}}{\sqrt{(1-K_H^2)^2+4K_H^2\left(\frac{z^2}{a^2}\right)}}\right] \qquad (77)$$

where the plus and minus signs are taken as in equations (51) and (53).

The integrated lift, side force, and rolling moment on an elemental strip are

$$\frac{d}{dx}\left(\frac{L}{q}\right)q=4\pi\alpha qs\frac{ds}{dx}\sigma_H; \qquad \frac{d}{dx}\left(\frac{Y}{q}\right)q=-4\pi\beta qt\frac{dt}{dx}\sigma_V \qquad (78)$$

$$\frac{d}{dx}\left(\frac{L'}{q}\right)q=2\alpha\beta q(t^2\tau_V-s^2\tau_H) \qquad (79)$$

where σ and τ are constants given by

$$\sigma=1+K^4+\frac{1}{2\pi}\left[2K(1-K^2)-(1+K^2)^2\sin^{-1}\frac{2K}{1+K^2}\right]$$

$$\tau=2K(1-K^2)+\pi(1+K^4)-(1+K^2)^2\cos^{-1}\frac{1-K^2}{1+K^2}$$

The subscripts H and V on σ and τ refer to the use of K_H or K_V in the above expressions. The lift, side-force, and rolling-moment coefficients for the entire conical cruciform-wing and body combination are then

$$C_L=\frac{\pi}{2}A_H\alpha\sigma_H \qquad C_Y=-\frac{\pi}{2}A_V\beta\sigma_V \qquad (80)$$

$$C_l=\frac{\alpha\beta}{3}\left(\tau_V\frac{t_0^2}{s_0^2}-\tau_H\right) \qquad (81)$$

Due to the radial nature of the lines of constant pressure, the center-of-pressure positions of both the lift and side forces are independent of the body-radius wing-semispan ratios and lie at the two-thirds chord point. The pitching and yawing moments are then given by

$$C_m=-\frac{\pi}{3}A_H\alpha\sigma_H \qquad C_n=\frac{\pi}{3}A_V\beta\sigma_V \qquad (82)$$

The lift, side-force, pitching-moment, and yawing-moment results are plotted in figures 4 and 5. Figure 9 presents

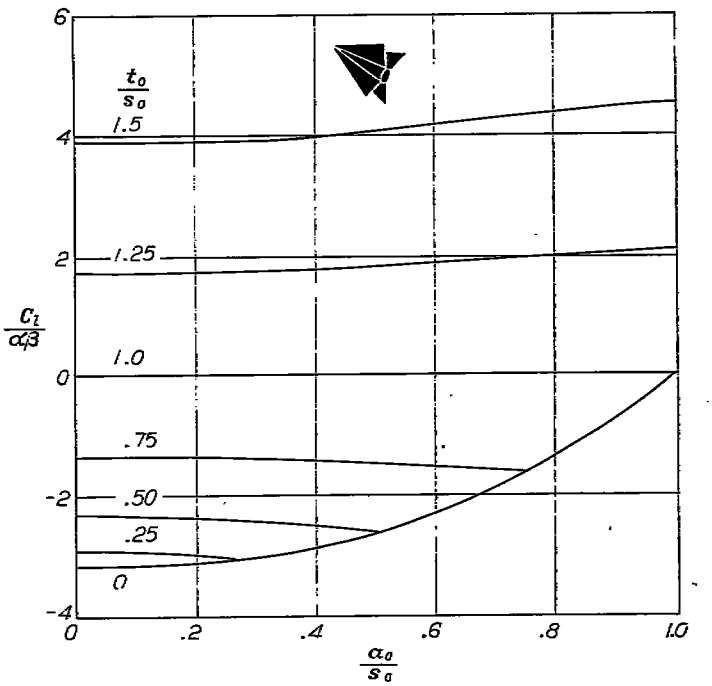

FIGURE 9.—Rolling moment for conical cruciform-wing and body combinations.

rolling-moment results for selected ratios of vertical wing span to horizontal wing span. To facilitate the computation of further results, the values of τ for use in equation (81) are plotted as a function of K in figure 10.

Triangular cruciform wings on an infinite cylinder.—The next example to be considered is that of a triangular cruciform wing mounted on an infinite cylindrical body. The essential relationships associated with this configuration are that

$$a=a_0; \qquad \frac{da}{dx}=0$$

and that ds/dx and dt/dx are positive constants. As with the corresponding case for plane-wing and body combinations, no forces are exerted on the body at stations ahead of the most forward or aft of the most rearward part of the wings.

Between these stations, forces are exerted on the wings and body in accordance with the following relations:

$$\left(\frac{\Delta p_L}{q}\right)_H=4\alpha\left[\frac{\frac{ds}{dx}\left(1-\frac{a_0^4}{s^4}\right)+\beta\frac{y}{s}\left(1-\frac{a_0^4}{y^4}\right)}{\sqrt{\left(1+\frac{a_0^4}{s^4}\right)-\frac{y^2}{s^2}\left(1+\frac{a_0^4}{y^4}\right)}}\right]$$

$$\left(\frac{\Delta p_L}{q}\right)_B=4\alpha\left[\frac{\frac{ds}{dx}\left(1-\frac{a_0^4}{s^4}\right)+4\beta\frac{y}{s}\left(1-\frac{y^2}{a_0^2}\right)}{\sqrt{\left(1+\frac{a_0^2}{s^2}\right)^2-4\frac{y^2}{s^2}}}\right]\pm\frac{16\alpha\beta\frac{y^2}{a_0 t}\sqrt{1-\frac{y^2}{a_0^2}}}{\sqrt{\left(1-\frac{a_0^2}{t^2}\right)^2+4\frac{y^2}{t^2}}}$$

$$\left(\frac{\Delta p_Y}{q}\right)_V=4\beta\left[\frac{-\frac{dt}{dx}\left(1-\frac{a_0^4}{t^4}\right)+\alpha\frac{z}{t}\left(1-\frac{a_0^4}{z^4}\right)}{\sqrt{\left(1+\frac{a_0^4}{t^4}\right)-\frac{z^2}{t^2}\left(1+\frac{a_0^4}{z^4}\right)}}\right]$$

$$\left(\frac{\Delta p_Y}{q}\right)_B=4\beta\left[\frac{-\frac{dt}{dx}\left(1-\frac{a_0^4}{t^4}\right)+4\alpha\frac{z}{t}\left(1-\frac{z^2}{a_0^2}\right)}{\sqrt{\left(1+\frac{a_0^2}{t^2}\right)^2-4\frac{z^2}{t^2}}}\right]\pm\frac{16\alpha\beta\frac{z^2}{a_0 s}\sqrt{1-\frac{z^2}{a_0^2}}}{\sqrt{\left(1-\frac{a_0^2}{s^2}\right)^2+4\frac{z^2}{s^2}}} \tag{83}$$

where the plus and minus signs are taken as in equations (51) and (53).

The integrated forces and moments on an elemental strip are given by

$$\frac{d}{dx}\left(\frac{L}{q}\right)q=4\pi\alpha q s\left(1-\frac{a_0^4}{s^4}\right)\frac{ds}{dx};\qquad \frac{d}{dx}\left(\frac{Y}{q}\right)q=-4\pi\beta q t\left(1-\frac{a_0^4}{t^4}\right)\frac{dt}{dx} \tag{84}$$

$$\frac{d}{dx}\left(\frac{L'}{q}\right)q=2\alpha\beta q t^2\left[2\frac{a_0}{t}\left(1-\frac{a_0^2}{t^2}\right)+\pi\left(1+\frac{a_0^4}{t^4}\right)-\left(1+\frac{a_0^2}{t^2}\right)^2\cos^{-1}\frac{t^2-a_0^2}{t^2+a_0^2}\right]-$$
$$2\alpha\beta q s^2\left[2\frac{a_0}{s}\left(1-\frac{a_0^2}{s^2}\right)+\pi\left(1-\frac{a_0^4}{s^4}\right)-\left(1+\frac{a_0^2}{s^2}\right)^2\cos^{-1}\frac{s^2-a_0^2}{s^2+a_0^2}\right] \tag{85}$$

The force and moment coefficients are found by integration to be

$$C_L=\frac{\pi}{2}A_H\alpha\left(1-\frac{a_0^2}{s_0^2}\right)^2;\qquad C_Y=-\frac{\pi}{2}A_V\beta\left(1-\frac{a_0^2}{t_0^2}\right)^2 \tag{86}$$

$$\left.\begin{aligned}C_m&=-\frac{\pi}{6}A_H\alpha\left[\left(1-\frac{a_0}{s_0}\right)^2\left(2+3\frac{a_0}{s_0}+3\frac{a_0^2}{s_0^2}\right)\right]\\ C_n&=\frac{\pi}{6}A_V\beta\left[\left(1-\frac{a_0}{t_0}\right)^2\left(2+3\frac{a_0}{t_0}+3\frac{a_0^2}{t_0^2}\right)\right]\end{aligned}\right\} \tag{87}$$

$$C_l=\frac{\alpha\beta}{3}\left(\frac{S_V t_0}{S_H s_0}\nu_V-\nu_H\right) \tag{88}$$

where

$$\nu=2K(1-K^2)+\pi(1+4K^3-3K^4)-(1+6K^2-K^4)\cos^{-1}\frac{1-K^2}{1+K^2}+\frac{7}{3}K^3\log\frac{2K^2}{1+K^2}$$

where, for determining ν_V, K is taken as a_0/t_0 and, for ν_H, K is taken as a_0/s_0. In equation (87), the moments are taken about the leading edge of the root chord. The lift, side-force, pitching-moment, and yawing-moment results are plotted in figures 4 and 5. The rolling-moment results cannot be plotted in general, however, as was done in the case of the preceding example since there are now three significant parameters instead of two. To facilitate calculation of these results, therefore, the variation of ν with K has been plotted in figure 10. As was shown in general, the rolling moment vanishes when the two wings become identical.

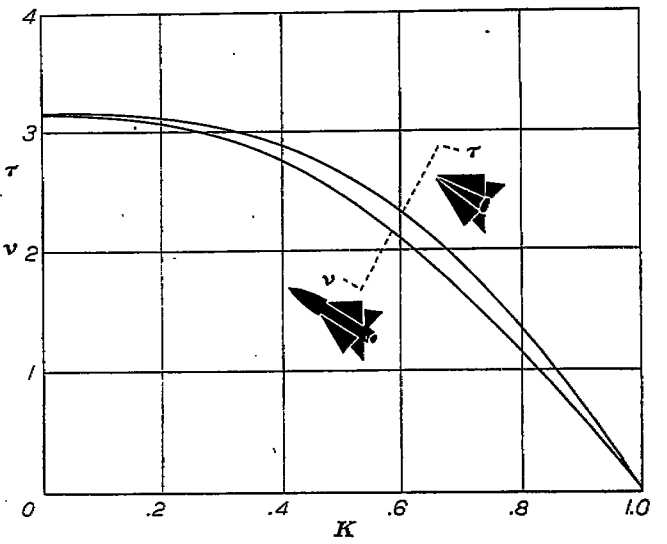

FIGURE 10.—Variation of τ and ν with K.

Triangular cruciform wings on a pointed body.—The theoretical characteristics of a triangular cruciform wing mounted on a pointed body of revolution, closed in an arbitrary manner at the nose but cylindrical along the wing root, may be determined by combining the results of two previous examples. The portion of the wing-body combination ahead of the leading edge of the wing root may be considered to be equivalent to the arbitrary body of revolution treated in the second example. The portion of the wing-body combination aft of the leading edge of the wing root is equivalent to a

fore evaluated by integrating the first bracketed term over the entire projected area of the wing-body combination.

$$L=\rho V_0\alpha\int_{B,H}\int\left[\left(\frac{\partial\phi'_a}{\partial x}\right)_u-\left(\frac{\partial\phi'_a}{\partial x}\right)_l\right]dxdy \tag{94}$$

The pitching moment is given similarly by

$$M=-\rho V_0\alpha\int_{B,H}\int\left[\left(\frac{\partial\phi'_a}{\partial x}\right)_u-\left(\frac{\partial\phi'_a}{\partial x}\right)_l\right]xdxdy \tag{95}$$

An expression for the rolling moment due to lifting differential pressures may be obtained in a similar manner. The first and third bracketed terms in equation (93) need not be considered; the first because it is even in y, the third because it is different from zero only on the surface of the body. Hence, the rolling moment due to the lifting differential pressure is given by

$$L'_L=+\rho V_0\beta\int\int_H\left[\left(\frac{\partial\phi'_a}{\partial y}\right)_u-\left(\frac{\partial\phi'_a}{\partial y}\right)_l\right]ydxdy \tag{96}$$

where the integration is carried over only the area of the horizontal wing.

In a similar manner, expressions for the side force, yawing moment, and rolling moment may be developed from the differential pressure between corresponding points on the port and starboard sides of the wing-body combination, thus

$$Y=\rho V_0\beta\int_{B,V}\int\left[\left(\frac{\partial\phi'_b}{\partial x}\right)_p-\left(\frac{\partial\phi'_b}{\partial x}\right)_s\right]dxdz \tag{97}$$

$$N=-\rho V_0\beta\int_{B,V}\int\left[\left(\frac{\partial\phi'_b}{\partial x}\right)_p-\left(\frac{\partial\phi'_b}{\partial x}\right)_s\right]xdxdz \tag{98}$$

$$L'_Y=-\rho V_0\alpha\beta\int\int_V\left[\left(\frac{\partial\phi'_b}{\partial z}\right)_p-\left(\frac{\partial\phi'_b}{\partial z}\right)_s\right]zdxdz \tag{99}$$

where the integration is carried over the projected area of the wing-body combination in equations (97) and (98) and only over the area of the vertical wing in equation (99).

The total rolling moment is

$$L'=L'_L+L'_Y=\rho V_0\alpha\beta\left\{\int\int_H\left[\left(\frac{\partial\phi'_a}{\partial y}\right)_u-\left(\frac{\partial\phi'_a}{\partial y}\right)_l\right]ydxdy-\int\int_V\left[\left(\frac{\partial\phi'_b}{\partial z}\right)_p-\left(\frac{\partial\phi'_b}{\partial z}\right)_s\right]zdxdz\right\}=0 \tag{100}$$

since it can be seen that the two integrals have identical values because the flows they represent are identical save for orientation in the coordinate system.

From examination of equations (94) through (100), it may be seen that the aerodynamic properties of cruciform-wing and body combinations having identical vertical and horizontal wings of arbitrary plan form and aspect ratio may be summarized in the following statements. The lift and pitching moment are independent of the angle of yaw and the side force and yawing moment are independent of the angle of attack. Further, the rolling moment is zero for all combinations of angles of pitch and yaw. For the corresponding problem relating to a cruciform-wing and body combination inclined in pitch and bank, the conclusions may be restated as follows: The lift and longitudinal center-of-pressure position are independent of the angle of bank and the rolling moment is zero for all angles of bank.

It should be noted that the value of zero for the rolling moment in the case of identical wings results from a complete balancing of the rolling moment exerted on the horizontal wing by an equal but opposite rolling moment on the vertical wing rather than by having zero rolling moment on each wing. Since such a complete balancing may be easily disturbed by factors neglected in the analysis (for instance, higher-order terms neglected in the analysis [1] or separation along the wing-body junction), particularly at large angles of inclination, the pitch and yaw range over which this conclusion is expected to apply may be more limited than that of the conclusions regarding lift and side force.

CONCLUDING REMARKS

An analysis has been made and expressions have been developed for the load distribution, forces, and moments on inclined plane- and cruciform-wing and body combinations consisting of a slender body of revolution and low-aspect-ratio pointed wings.

These results indicate four general characteristics of slender cruciform-wing and body combinations. First, there is a complete correspondence of the expressions for the lift and side force. Second, the lift is independent of the angle of yaw and the side force is independent of the angle of attack. Third, the expressions for the lift and pitching moment for slender cruciform-wing and body combinations are identical to those for slender plane-wing and body combinations. Last, if the vertical and horizontal wings are identical, the rolling moment is zero. For the corresponding problem relating to cruciform-wing and body combinations inclined in pitch and bank these conclusions may be restated in the following manner. The lift and pitching moment are independent of the angle of bank and the rolling moment is zero for all angles of bank. It is further shown, by symmetry considerations that these conclusions are applicable to any wing-body combination having identical horizontal and vertical wings of arbitrary plan form and aspect ratio.

[1] Maple and Synge (reference 19) have shown that inclusion of higher-order terms results in rolling moments proportional to the fourth and larger powers of the angle of inclination.

AMES AERONAUTICAL LABORATORY,
NATIONAL ADVISORY COMMITTEE FOR AERONAUTICS,
MOFFETT FIELD, CALIF., *Mar. 24, 1949.*

cruciform arrangement of triangular wings mounted on an infinite cylinder discussed in the preceding example. The load distribution and integrated load on an elemental spanwise strip are then the same as those given in the corresponding example.

The lift and side-force coefficients are found by adding the forces on the component parts of the wing-body combination and dividing by the dynamic pressure and the characteristic area. The lift and side-force coefficients are then

$$C_L=\frac{\pi}{2}A_H\alpha\left(1-\frac{a_0^2}{s_0^2}+\frac{a_0^4}{s_0^4}\right);\qquad C_Y=-\frac{\pi}{2}A_V\beta\left(1-\frac{a_0^2}{t_0^2}+\frac{a_0^4}{t_0^4}\right). \tag{89}$$

These relationships are shown graphically in figure 4.

The pitching- and yawing-moment coefficients for this wing-body combination may be found in a manner similar to that used in finding the lift and side-force coefficients, taking care to transfer the moments of both components to the same axis, namely, the leading edge of the root chord.

$$\left.\begin{aligned}C_m&=-\frac{\pi A_H\alpha}{6}\left[\left(1-\frac{a_0}{s_0}\right)^2\left(2+3\,\frac{a_0}{s_0}+\frac{a_0^2}{s_0^2}\right)\right]+2\alpha\,\frac{B_m}{S_H}\,\frac{l}{c_H}\\ C_n&=+\frac{\pi A_V\beta}{6}\left[\left(1-\frac{a_0}{t_0}\right)^2\left(2+3\,\frac{a_0}{t_0}+\frac{a_0^2}{t_0^2}\right)\right]-2\beta\,\frac{B_m}{S_V}\,\frac{l}{c_V}\end{aligned}\right\} \tag{90}$$

The rolling-moment coefficient is given, of course, by equation (88).

GENERAL CRUCIFORM-WING AND BODY COMBINATIONS HAVING IDENTICAL WINGS

The analysis of slender cruciform-wing and body combinations resulted in the discovery of certain general characteristics of wing-body combinations having identical vertical and horizontal wings. It is the purpose of this section to enlarge the range of configurations to which these conclusions are applicable by removing the requirement of slenderness. To accomplish this, an analysis of the aerodynamic forces and moments exerted on cruciform-wing and body combinations having identical wings will be undertaken on the basis of symmetry considerations. For this treatment the wings may be of any plan form or aspect ratio; provided the vertical and horizontal wings are identical and are mounted at the same longitudinal position of the body. The concepts of linearized theory are used in this treatment; therefore, the usual restrictions that the body is slender and that the angles of pitch and yaw are small must be observed. The conclusions are applicable at all speeds, since the Mach number does not enter the problem directly. Consider the cruciform-wing and body combinations as being inclined small angles α in pitch and β in yaw from the free-stream direction, the free-stream velocity being V_0. Since superposition is a valid principle in linearized theory, the perturbation velocity potential ϕ may be considered to be the sum of the two components

$$\phi=\alpha\phi'_a+\beta\phi'_b \tag{91}$$

where ϕ'_a and ϕ'_b are the perturbation velocity potentials of the flow about a cruciform-wing and body combination, inclined unit angles of pitch and yaw, respectively.

Consider now the differential pressure between corresponding points on the upper and lower surfaces of the body and the horizontal wing

$$\begin{aligned}\frac{\Delta p_L}{q}=\frac{2}{V_0}\Bigg[&\left\{\alpha\left[\left(\frac{\partial\phi'_a}{\partial x}\right)_u-\left(\frac{\partial\phi'_a}{\partial x}\right)_l\right]+\beta\left[\left(\frac{\partial\phi'_b}{\partial x}\right)_u-\left(\frac{\partial\phi'_b}{\partial x}\right)_l\right]\right\}-\\ &\beta\left\{\alpha\left[\left(\frac{\partial\phi'_a}{\partial y}\right)_u-\left(\frac{\partial\phi'_a}{\partial y}\right)_l\right]+\beta\left[\left(\frac{\partial\phi'_b}{\partial y}\right)_u-\left(\frac{\partial\phi'_b}{\partial y}\right)_l\right]\right\}+\\ &\alpha\left\{\alpha\left[\left(\frac{\partial\phi'_a}{\partial z}\right)_u-\left(\frac{\partial\phi'_a}{\partial z}\right)_l\right]+\beta\left[\left(\frac{\partial\phi'_b}{\partial z}\right)_u-\left(\frac{\partial\phi'_b}{\partial z}\right)_l\right]\right\}\Bigg]\end{aligned} \tag{92}$$

Ordinarily, only the potential gradients, or perturbation velocities, in the x direction would be included in equation (92). For long slender objects, however, the perturbation velocities in the x direction are so much smaller than those in the y and z directions that the products of small angles and perturbation velocities in the y and z directions must be retained as well as the perturbation velocities in the x direction. Since the inclusion of these terms does not introduce any particular restrictions into the problem, they will be retained throughout the present discussion even though in many instances, such as with high-aspect-ratio unswept wings, it is unnecessary to do so. In general, none of the individual terms in equation (92) is zero and the pressure at every point depends upon both ϕ'_a and ϕ'_b, or, what is equivalent, upon both the angle of attack and the angle of of yaw. However, several of the terms are equal and will cancel. Thus, remembering that equation (92) represents the lifting differential pressure, it is apparent from symmetry considerations that

$$\left(\frac{\partial\phi'_b}{\partial x}\right)_u-\left(\frac{\partial\phi'_b}{\partial x}\right)_l=0;\qquad \left(\frac{\partial\phi'_b}{\partial y}\right)_u-\left(\frac{\partial\phi'_b}{\partial y}\right)_l=0;$$
$$\left(\frac{\partial\phi'_a}{\partial z}\right)_u-\left(\frac{\partial\phi'_a}{\partial z}\right)_l=0$$

everywhere and that

$$\left(\frac{\partial\phi'_b}{\partial z}\right)_u=\left(\frac{\partial\phi'_b}{\partial z}\right)_l=0$$

on the horizontal wing. Therefore, equation (92) simplifies to

$$\begin{aligned}\frac{\Delta p_L}{q}=\frac{2}{V_0}\Bigg\{&\underbrace{\alpha\left[\left(\frac{\partial\phi'_a}{\partial x}\right)_u-\left(\frac{\partial\phi'_a}{\partial x}\right)_l\right]}_{1}-\\ &\underbrace{\alpha\beta\left[\left(\frac{\partial\phi'_a}{\partial y}\right)_u-\left(\frac{\partial\phi'_a}{\partial y}\right)_l\right]}_{2}+\underbrace{\alpha\beta\left[\left(\frac{\partial\phi'_b}{\partial z}\right)_u-\left(\frac{\partial\phi'_b}{\partial z}\right)_l\right]}_{3}\Bigg\}\end{aligned} \tag{93}$$

where the third bracketed term differs from zero only on the body. The second and third bracketed terms are odd in y; hence, they cannot contribute to the lift. The lift is there-

REFERENCES

1. Lennertz, J.: On the Mutual Reaction of Wings and Body. NACA TM 400, 1927.
2. Wieselsberger, C., and Lennertz, J.: Airplane Body (Nonlifting System) Drag and Influence on Lifting System. Influence of the Airplane Body on the Wings. Aerodynamic Theory, vol. IV, div. K, ch. III, W. F. Durand, ed., Julius Springer (Berlin), 1935.
3. Pepper, Perry A.: Minimum Induced Drag in Wing-Fuselage Interference. NACA TN 812, 1941.
4. Multhopp, H.: Aerodynamics of the Fuselage. NACA TM 1036, 1942.
5. Spreiter, John R.: Aerodynamic Properties of Slender Wing-Body Combinations at Subsonic, Transonic, and Supersonic Speeds. NACA TN 1662, 1948.
6. Spreiter, John R.: Aerodynamic Properties of Cruciform-Wing and Body Combinations at Subsonic, Transonic, and Supersonic Speeds. NACA TN 1897, 1949.
7. Munk, Max. M.: The Aerodynamic Forces on Airship Hulls. NACA Rep. 184, 1924.
8. Jones, Robert T.: Properties of Low-Aspect-Ratio Pointed Wings at Speeds Below and Above the Speed of Sound. NACA Rep. 835, 1946.
9. Ribner, Herbert S.: The Stability Derivatives of Low-Aspect-Ratio Triangular Wings at Subsonic and Supersonic Speeds. NACA TN 1423, 1947.
10. Heaslet, Max. A., Lomax, Harvard, and Spreiter, John R.: Linearized Compressible-Flow Theory for Sonic Flight Speeds. NACA Rep. 956, 1950. (Formerly NACA TN 1824, 1949.)
11. Glauert, H.: The Elements of Aerofoil and Airscrew Theory. Cambridge Univ. Press, 2d ed., 1947.
12. Krienes, Klaus.: The Elliptic Wing Based on the Potential Theory. NACA TM 971, 1941.
13. Robinson, A., and Young, A. D.: Note on the application of the Linearized Theory for Compressible Flow to Transonic Speeds. Rep. No. 2, College of Aeronautics, Cranfield, Eng., 1947.
14. Robinson, A.: Aerofoil Theory of a Flat Delta Wing at Supersonic Speeds. Rep. No. Aero. 2151, R. A. E. (British), 1946.
15. Stewart, H. J.: The Lift of a Delta Wing at Supersonic Speeds. Quart. App. Math., vol. 4, no. 3, Oct. 1946, pp. 246–254.
16. Brown, Clinton E.: Theoretical Lift and Drag of Thin Triangular Wings at Supersonic Speeds. NACA Rep. 839, 1946.
17. Browne, S. H., Friedman, L., and Hodes, I.: A Wing-Body Problem in a Supersonic Conical Flow. Jour. Aero. Sci., vol. 15, no. 8, Aug. 1948, pp. 443–452.
18. von Kármán, Th., and Burgers, J. M.: General Aerodynamic Theory-Perfect Fluids. Aerodynamic Theory, vol. II, W. F. Durand, ed., Julius Springer (Berlin), 1935.
19. Maple, C. G., and Synge, J. L.: Aerodynamic Symmetry of Projectiles. Quart. App. Math., vol. VI, no. 4, Jan. 1949, pp. 345–367.

956646—51——20